

Journal of Materials Chemistry B

Accepted Manuscript



This is an *Accepted Manuscript*, which has been through the Royal Society of Chemistry peer review process and has been accepted for publication.

Accepted Manuscripts are published online shortly after acceptance, before technical editing, formatting and proof reading. Using this free service, authors can make their results available to the community, in citable form, before we publish the edited article. We will replace this *Accepted Manuscript* with the edited and formatted *Advance Article* as soon as it is available.

You can find more information about *Accepted Manuscripts* in the [Information for Authors](#).

Please note that technical editing may introduce minor changes to the text and/or graphics, which may alter content. The journal's standard [Terms & Conditions](#) and the [Ethical guidelines](#) still apply. In no event shall the Royal Society of Chemistry be held responsible for any errors or omissions in this *Accepted Manuscript* or any consequences arising from the use of any information it contains.



Journal Name

ARTICLE

Microfluidic Synthesis of QD-Encoded PEGDA Microspheres for Suspension Assay

Huan Liu^{a,b}, Xiang Qian,^a Zhenjie Wu^{a,b}, Rui Yang^a, Shuqing Sun^{a,b*}, Hui Ma^{a,b}

Received 00th January 20xx,
Accepted 00th January 20xx

DOI: 10.1039/x0xx00000x

www.rsc.org/

Uniform and size-controllable QD-encoded poly(ethylene glycol) diacrylate (PEGDA) microbeads were produced using a microfluidic device followed by in-situ photopolymerization. An S-shaped and gradually widening channel was designed to allow optimized UV exposure for photopolymerization and prevent coalescence. The as-obtained PEGDA microbeads exhibited well-defined sphericity and excellent monodispersity with coefficient of variation (CV) below 5 %, and the size varied from 7 μm to 120 μm can be selectively achieved by simply adjusting the experimental parameters. The fluorescence performance of the QDs was well reserved without significant peak broadening or distortion. Seven barcode libraries were realized with bright fluorescence and distinguished coding signals, which could be conveniently decoded by a flow cytometer. Furthermore, a very facile strategy to conjugate biomolecules on the bead surfaces was developed using polydopamine (PDA). A sandwich immunoassay of rabbit IgG was performed and the applicability of the QD-encoded microbeads for suspension assay was demonstrated.

Introduction

The rapid development of clinical diagnostics and drug discovery has led to urgent demand for a high throughput assay. This technology needs simultaneously detect multiple analytes within a small sample.¹⁻³ Many multiplexing technologies have been developed, mainly including planar assay^{4,5} and suspension assay.^{6,7} The planar assay is a position encoding method that immobilizes probe molecules on flat solid supports. Although this planar technique has an important impact on the analysis of ultrahigh-density, it has limitations on reaction rate, quantitative detection and flexibility. To address above problems, suspension assay based on barcode particles for tracking analytes becomes an attractive multiplex assay. It offers many advantages such as faster binding kinetics, flexibility in target selection and high quality of results. Three key issues are involved in the suspension assay: (i) effective encoding schemes to generate a sufficient number of accurate barcodes; (ii) the facile approach of coupling probes to the surface of encoded microcarriers; (iii) the conveniently decoding processes.^{8,9}

Various coding schemes, including spectral barcode,^{6,10-12} chemical barcode,¹³ graphical barcode,¹⁴ surface enhanced Raman scattering (SERS) barcode¹⁵ and so on, have been proposed. Owing to the excellent decoding ability with the

help of flow cytometers or fluorescence spectrometer, spectral encoding is more popular for multiplexed detection than other schemes. In the spectral coding process, the microspheres are generally encoded by fluorescence elements with different wavelengths and intensities to generate sufficient identification codes. Organic dye-based barcodes have been applied in commercial suspension array. However, organic dyes suffer from several disadvantages such as multiple excitation light sources, broad emission spectrum and photobleaching. As an alternative, quantum dot (QD) exhibited excellent optical properties such as narrow emission spectra, broad excitation wavelength, tunable size and high quantum yields.¹⁶⁻¹⁹ Especially, it can be easily decoded by modern flow cytometer.¹² These characteristics enable QD promising candidates for commercial application of suspension assays.

Many approaches of preparing QD-encoded microbeads have been developed, including swelling method,²⁰ layer-by-layer self-assembly method^{21,22} and copolymerization.^{23,24} Despite the progress these methods have made for generating QD barcodes, many challenges still remain, such as poor loading capacity, complicated process and QDs leakage. Recently, microfluidic technology has been used as an effective approach to create barcode microspheres.²⁵⁻³⁴ However, it has been challenging to precisely control the size of the microbeads over a wide range and a common method to modify the bead surfaces for further application was still needed.

How to conveniently conjugate probe (protein or DNA et al) to the surface of encoded beads is an important issue. Dopamine is the main ingredient secreted by the foot antennae of marine organisms—mussel, which can be adhered

^a Institute of optical imaging and sensing, Shenzhen Key Laboratory for Minimal Invasive Medical Technologies, Graduate School at Shenzhen, Tsinghua University, Shenzhen 518055, China

^b Department of Physics, Tsinghua University, Beijing 100084, China

* To whom correspondence should be addressed. Email: sun.shuqing@sz.tsinghua.edu.cn

to almost all wet surfaces of organic and inorganic materials through oxidative self-polymerization. More importantly, polydopamine (PDA), a kind of environment friendly biopolymer, could provide ample active catechol and amine groups for the attachment of biomolecules.³⁵⁻³⁷ In this study, we developed a facile approach for the preparation of QD-doped barcodes using microfluidic technology. Size-controllable and uniform microbeads were produced through adjusting the flow conditions. Different QDs were incorporated into PEGDA beads by simply mixing them together prior to injection, and their fluorescent properties were investigated. The resulted barcodes exhibit good spectral characteristics and accurate coding capability. In addition, the PDA-modified barcodes were used for the detection of rabbit-IgG and decoded by flow cytometer. We expect the combination of microfluidic generation of microbeads with PDA modification strategy will provide a general approach for the development of suspension array technology.

Experimental

Microfluidic Devices

A silicon master was fabricated with SU8-2015 photoresists using photolithography, and a microfluidic device was obtained with polydimethylsiloxane (PDMS, RTV615, Momentive, USA) embossing from the silicon master. After solidification, the PDMS replica was bonded to a 25 mm by 75 mm glass substrate following oxygen plasma treatment of both surfaces.

Preparation of QD/mPEG-SH Nanocrystals

Core-shell CdSe/ZnS QDs (3.5 mg/mL) with emission peak at 525 nm and 625 nm were purchased from Wuhan Jiayuan Quantum Dots (China). They were coated with a mixture of HDA and TOPO and dispersed in *n*-hexane. Methoxy PEG Thiol (mPEG-SH, MW 5000, JenKem Technology Co., China) was used to modify the above mentioned QDs. In brief, 5 mg of mPEG-SH was added into 1 mL QD solution and mixed with 3 mL of PEGDA solution, the mixture was kept at room temperature for 12 h before use.

Preparation of the QD-embedded Microbeads

The disperse phase was the hydrophilic poly(ethylene glycol) diacrylate (PEGDA, MW 250, Sigma-Aldrich) containing appropriate QDs. And 2-Hydroxy-4'-(2-hydroxyethoxy)-2-methylpropiophenone (98%, MW 224, Tci) at concentration of 5 mg/mL was added to the disperse phase as the photoinitiator. The continuous phase was prepared by dissolving 4 wt % of surfactants (EM 90, ABIL) in Hexadecane (99%, Sigma-Aldrich). Disperse and continuous fluids were introduced into the microfluidic device through a polytetrafluoroethylene tube, and the flow rates were controlled using two syringe pumps (LSP01-1A, Baoding Longer Precision Pump Co.) and gastight syringes. Emulsion droplets can be fabricated by adjusting the flow rates, and monodispersed QDs-embedded microbeads can be produced

by photopolymerizing the monomer emulsion droplets in situ using a UV lamp (365 nm, LED SPOT LIGHT SOURCE, FUTANSI.). The final products were kept in a vacuum and dried in oven overnight (50 °C, around 0.1 MPa) for further application.

Preparation of PEGDA-PDA Composite Spheres

Dopamine (DA, 99%, Alfa Aesar) with various concentrations (0.5 mg/mL, 1mg/mL, 1.5 mg/mL, 2mg/mL and 4mg/mL) were prepared by dissolving dopamine in Tris-HCl buffer solution (10 mM, pH = 8.5). Next, the PEGDA microspheres were added to the dopamine solution and the mixture was stirred for 24 h at room temperature. The as-prepared composite spheres were washed several times using deionized water before further use.

QD-Encoded Microbead-Based Sandwich Immunoassays

There were mainly three steps for QD-encoded microbead-based sandwich immunoassays. First, capture antibody goat anti-rabbit IgG (Beijing 4A Biotech Co., Ltd, China) was immobilized on the surface of PEGDA-PDA microspheres encoded with QD-625nm: 5 mg of QD-doped PEGDA-PDA beads were suspended in 500 μ L PBS solution (0.01M, pH 7.4) followed by addition of 50 μ L of goat anti-rabbit IgG (1 mg/ml in PBS), the mixture was incubated on a shaking table at room temperature for 2 h. The beads were washed three times using PBS and stored in 500 μ L of blocking solution (1 % BSA in PBS) overnight at 4 °C. Next, 200 μ L dispersion of the above microspheres (1 mg/ μ L) and 10 μ L of target antigen (rabbit IgG, 1 mg/mL, Sigma-Aldrich) were mixed in PBS for 1 h. The beads were washed three times with PBS and resuspended in 200 μ L of PBS. Finally, 10 μ L of reporter FITC-labeled goat anti-rabbit IgG (0.5 mg/ml, Southern Biotech, USA) was added into the above solution. The mixture was incubated on a shaker for 1 h and washed three times. The resulted beads were stored in 200 μ L of PBS for flow cytometer analysis. The control group was carried out in the same manner without addition of the target antigen.

Characterization

The optical micrographs of the microbeads were captured using a CCD camera mounted on an inverted microscope (Olympus IX2-UCB). The average size and the CV of the as-generated microbeads were determined by measuring at least 100 particles on each frame using image analysis software (Image-Pro Plus). The CV is defined by the following equation of $CV = \delta/d_{av} \times 100\%$, where δ is the standard deviation, and d_{av} is the average droplet diameter.

The fluorescence spectrums of QD-encoded microbeads were analyzed by a spectrofluorophotometer (RF-5301PC, SHIMADZU). The fluorescence images of the QD-doped barcode were captured by a fluorescence microscope (Olympus).

The scanning electron microscopy (SEM, S-4800, HITACHI) were used to acquire the surface morphology of the microbeads. The polymerization of PEGDA microspheres was confirmed by Fourier transform infrared spectroscopy (FTIR, Vertex-70, BRUKER). Thermogravimetric analysis (TGA) was

performed on a simultaneous thermal analyzer (METTLER TOLEDO, Switzerland) to confirm the content of PDA, all dried powder samples were heated from 30 °C to 700 °C with the rate of 10 °C/min under nitrogen environment. To perform FTIR, SEM and TGA, the microbeads were transferred from oil phase into n-hexane, followed by three cycles of centrifugation (200 rpm for 3 min). The microbeads were dried under vacuum overnight.

A flow cytometer (FACS Calibur, BD) was used to decode the QD-encoding microspheres. The samples were suspended in PBS solution. Green fluorescence was detected on the FL1 channel, yellow fluorescence and red fluorescence were collected on the FL2 channel and the FL3 channel, respectively. Beads were analyzed at up to 10000 events for each sample. A single light source at 488 nm was used to excite all fluorescence colors.

Results and discussion

Microfluidic generation of PEGDA beads

The microfluidic device for microbead preparation consists of two parts: a nozzle zone for the breakup of barcode droplets and a UV exposure zone used to solidify the microbeads by in-situ photopolymerization to ensure the monodispersity of microbeads, as shown in Figure 1a. In the nozzle zone, the disperse phase, PEGDA solution was connected to the microfluidic device from inlet A using a syringe pump, and the continuous phase hexadecane was injected from inlet B. Because photopolymerization requires plenty residence time and sufficient UV exposure, an S-shaped channel with gradually increasing width is designed for efficient photopolymerization and prevent coalescence. The formation process of a microsphere is recorded by CCD camera (Figure b1 – b8), and the particles were constructed through shearing the disperse phase by two steady continuous phases. This design is optimized for generating monodisperse PEGDA droplets and subsequent photopolymerization to produce robust PEGDA microbeads.

The factors that affect the droplets size mainly include the flow rate of disperse and continuous phase and the channel size. Here, the relationship between droplet diameter and flow rate was investigated. When the flow rate of continuous phase (Q_c) was maintained at 30 $\mu\text{L}/\text{min}$ and that of the disperse phase (Q_d) was set to 0.5, 1 and 2 $\mu\text{L}/\text{min}$, the droplet diameter were 10 μm , 18 μm and 39 μm , respectively, as shown in Figure 2(a-c). The resulted microspheres show narrow size distribution with CV below 5% and well-defined sphericity, which meet the basic requirement for accurate QD encoding by microfluidic technology. Figure 2e reveals that the size of microbeads decreases with the increase of Q_c when Q_d was maintained at 1 $\mu\text{L}/\text{min}$. In contrast, the size of microbeads increases with the increase of the flow rate of disperse phase when Q_c was set at 30 $\mu\text{L}/\text{min}$ (Figure 2f).

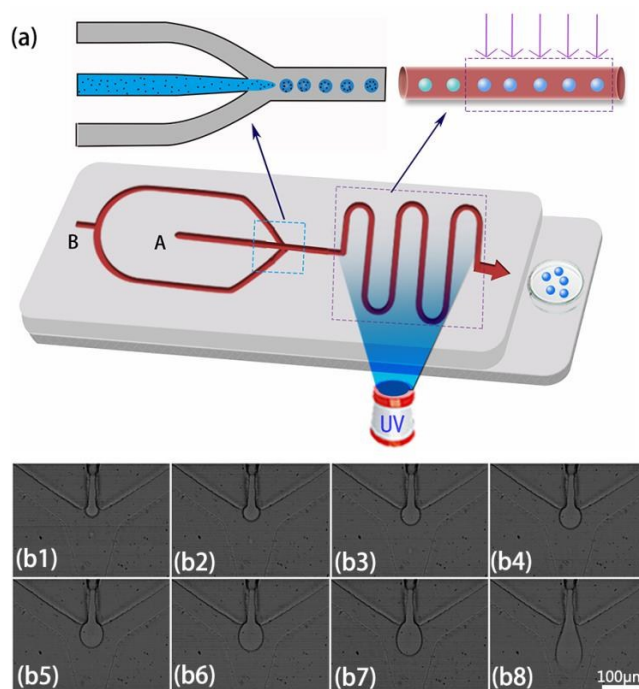


Figure 1. Schematic diagram of the flow-focusing microfluidic device and the typical droplet formation process in channel. (a) PEGDA droplets are produced in the nozzle zone, the disperse phase PEGDA solution is injected from inlet A and the continuous phase is imported from inlet B. The left inset is the enlargement of nozzle zone, the black dots in disperse phase represent QDs. The other part is the UV exposure zone with gradually widening snake shape channel for the in-situ polymerization of PEGDA droplets. The right inset shows the solidifying process of PEGDA beads in channel. (b) Optical micrographs of the generation process of a single droplet ($Q_c = 5 \mu\text{L}/\text{min}$ and $Q_d = 30 \mu\text{L}/\text{min}$). The scale bar is 100 μm .

UV-exposure not only polymerizes the monomer in the droplets in-situ, but resulted in the shrinkage of the microbeads. The dimensions of PEGDA microparticles were about 5–10% smaller than the corresponding monomer droplets after photopolymerization. FTIR spectroscopy was used to monitor the in-situ photopolymerization of PEGDA from liquid oligomer to robust insoluble microbeads in the microfluidic device. The droplets were formed in the cross area and then exposed to 365nm UV light in the S-shaped channel for less than 1 s. The activated radicals initiated the photopolymerization by attacking the carbon-carbon double bonds (C=C) presented in two acrylate groups of PEGDA, finally resulted in linear chain growth and cross-linked network. As shown in Figure 3a, the conversion of C=C was confirmed by comparing the peak of C=C stretch at 1630 cm^{-1} before and after photopolymerization. It revealed that the polymerization process was rapid and the conversion of double bonds almost completed. The higher level of conversion will increase the amount of volume change and the mechanical stability of the formed microspheres. The insets in Figure 3a show the typical SEM images of the microparticles after and before UV

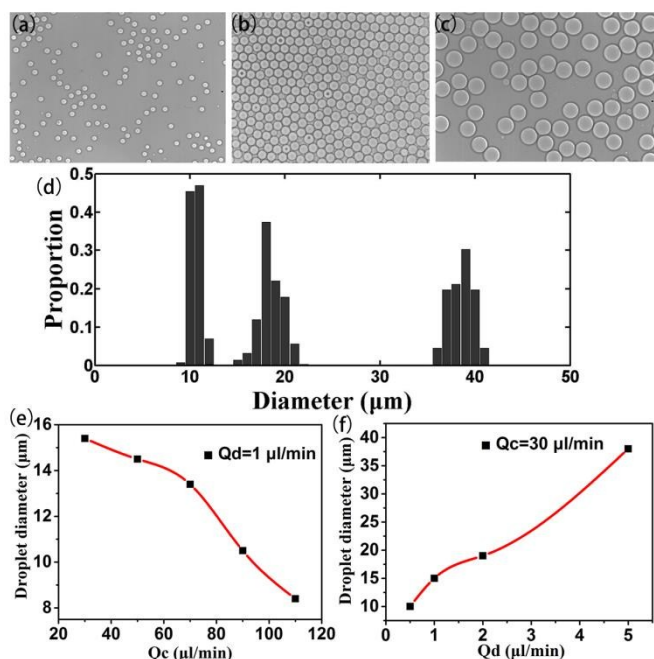


Figure 2. The typically optical images of PEGDA droplets and effects of flow rates on droplet diameter. (a) – (c) are the optical micrographs of uniform emulsions prepared by above microfluidic device. ($Q_c = 30 \mu\text{L} / \text{min}$; $Q_d = 0.5 \mu\text{L} / \text{min}$, $Q_d = 1 \mu\text{L} / \text{min}$ and $Q_d = 2 \mu\text{L} / \text{min}$, respectively). The scale bar is 50 μm . (d) Size distribution of the produced microparticles in (a) – (c). CV is below 5%. (e), (f) Dependence of average droplet diameter on the disperse-phase flow rate Q_d and the continuous-phase flow rate Q_c . The droplet diameter decreases with the increasing of Q_c , but increases with the increasing of Q_d . The average droplet size were determined by measuring the sizes of approximately 100 droplets on each frame.

exposure, respectively, which indicates the good sphericity of the microbeads can only maintained after sufficient polymerization. The SEM micrograph in Figure 3b confirms the uniformity and fine globular shape of the PEGDA polymer beads. So the resulted microbeads exhibit robust solid structure, which is important for the decoding process using a flow cytometer.

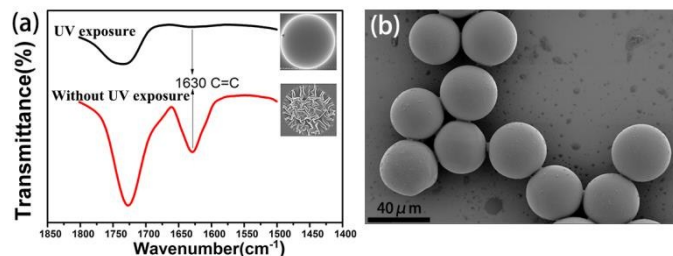


Figure 3. FTIR and SEM images. (a) FTIR spectra of PEGDA before and after UV exposure. The insets are the collapsed PEGDA droplet without UV exposure and the robust PEGDA microbead with abundant UV exposure to photopolymerization. (b) SEM image of PEGDA microbeads

verifying its robust structure. The bar scale is 40 μm .

QD-doped barcode beads

Every QD-doped microsphere can be recognized as a small library, because QDs with different emission wavelengths and intensities are trapped into microspheres to generate a large scale of barcodes according to the following formula: $C = N^m - 1$ (where C is barcode number, N is the number of intensity levels and m is the number of color). However, most of the developed incorporation methods suffer from several problems, including low coding capacity, long processing time and the waste of loading materials. In this study, it is easy to incorporate any color and intensity into the PEGDA bead by simply mixing them together as the disperse phase. Since the PEGDA is a hydrophilic polymer, the surface of CdSe/ZnS core-shell QDs was modified with mPEG-SH. As shown in Figure 4(a-c), single color QD-encoded microspheres were produced by using 525 nm, 572 nm and 625 nm QD, respectively. As we can see, QDs have been completely encapsulated in PEGDA microspheres and all particles show bright and uniform fluorescence.

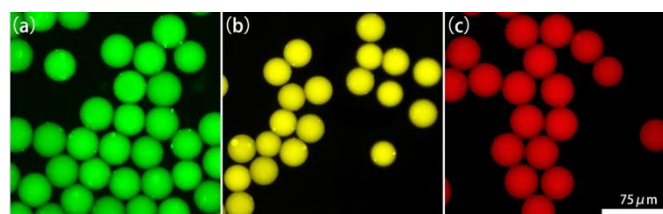


Figure 4. The fluorescence pictures of single color barcode microspheres. (a) – (c) The emission light of QD-embedded beads are 525 nm (green), 572 nm (yellow) and 625 nm (red).

In Figure 5a, the solid lines show fluorescence spectrum (normalized) of single color QD-encoded barcodes corresponding to Figure 4(a-c), in which QD-loaded beads show distinguished optical characteristics. The dotted lines represent fluorescent spectroscopy of the pure QDs dispersed in deionized water. The widths of spectrums are almost unchanged during doping process except that the emission maximum of QD-525 nm slightly red shifts 10 nm after trapped in microspheres. Although the emission maximum of QD slightly red shifted in microspheres compared with their fluorescence spectrum in aqueous solution, it doesn't show any effect on subsequent multiple coding. Figure 5(b-d) show individual images of four unique barcodes containing two color QDs with different intensities, using 572 nm and 625 nm QD. In principle, the fluorescence intensity of each QD-doped barcode is proportional to the molar concentration of every QD in disperse phase. This principle offers the theoretically possibility to create a huge number of barcodes through controlling concentrations in disperse phase solution. Here, in order to obtain the significant coding signals, we employ relative intensities to encode, and three different intensity levels were selected in the process, namely 1, 2 and 4.

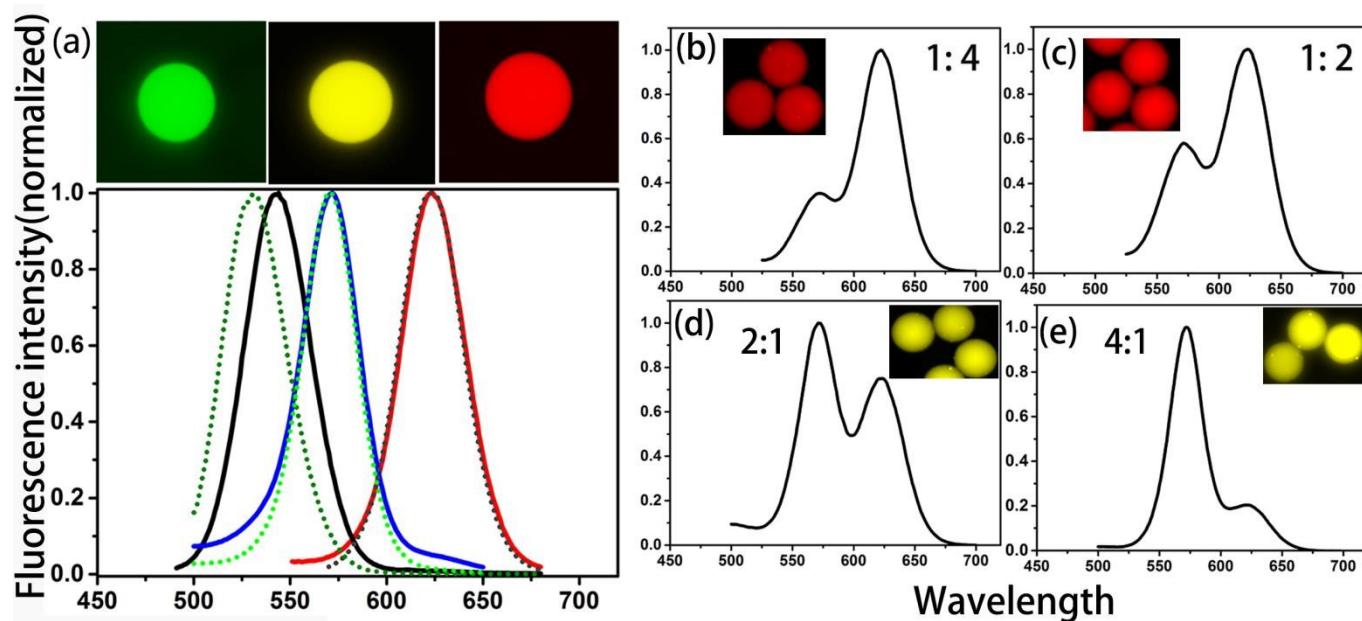


Figure 5. Seven barcode libraries. (a) The single color QD for encoding. The solid lines represent the spectrums of the single color barcodes. The dotted lines show the spectrum of original QDs diluting in water. The insets show the fluorescence microscope images of barcodes doped QD-525 nm, QD-572 nm and QD-625 nm. (b) – (e) Representative spectra of QDs-encoded beads containing two types of QDs 572:625 nm to create 1:4, 1:2, 2:1 and 4:1 coding signals. The insets are corresponding fluorescence images.

Through simply adjusting the QDs concentration in disperse phase, the barcode of 1:4, 1:2, 2:1 and 4:1 were successfully prepared with using the QDs combination of 572 nm and 625 nm. The resulted barcodes carried a serial of precise and distinct signals and did not exhibit spectral overlap and fluorescence resonance energy transfer phenomena, this may attribute to the surface of QD modified with mPEG-SH and QDs are compatible and dispersible in PEGDA solution. Therefore, the microfluidic strategy is effective to generate high quality fluorescent barcoded microbeads for multiplexed sensing applications.

Preparation and characterization of PEGDA/PDA composite microspheres

The microspheres used as the carrier for coding elements usually require carboxyl or amine groups on their surface, which can covalently attach protein or DNA with EDC and NHS as activators. Here, we developed a facile strategy to this end by coating PDA on the surface of PEGDA. The polydopamine coating layers have abundant active catechol and amine groups on their surface, which can facilitate secondary reactions without additional activators in this procedure. The surface morphologies of the PEGDA sphere and PEGDA-PDA sphere were recorded by SEM. Figure 6a shows the pure PEGDA spheres; its surface was nearly smooth. And Figure 6(b-f) show the PEGDA-PDA spheres prepared using different PDA concentrations, namely, 0.5, 1, 1.5, 2 and 4 mg/mL, respectively. One can find that the surface roughness increases with the increasing of PDA concentration. The PEGDA spheres modified with PDA under concentration of 2 mg/mL were selected for further characterization and attachment of

proteins.

Figure 6g shows the TGA results of PEGDA spheres and PEGDA-PDA composite spheres, which reveals their thermal stability. The pristine PEGDA spheres began to lose weight at about 310 °C and completely decomposed at around 430 °C. The residue weight percent of the pure PEGDA spheres should have reduced to 0% at a high temperature under anaerobic circumstances, but a little oxygen helped them burn away. After PEGDA beads were coated by a PDA layer, the PEGDA spheres started to lose weight at 370 °C and around 10 % residue substance were preserved as a result of the protection of PDA layer. This result also demonstrated the successful modification of PDA on PEGDA spheres.

Flow cytometry analysis of QD-encoded bead-based immunoassays

Using flow cytometer to decode QD-coded microbeads is a versatile approach to obtain their spectroscopic and size signals. Figure 7a and 7b indicate that the PEGDA microspheres have a narrow size distribution. Figure 7c is the fluorescence intensity comparison of PEGDA microspheres and QD-encoded microspheres and it indicates that QD-trapped beads are about 200 times brighter than PEGDA beads. The uniform size and bright fluorescence enable the QD-encoded PEGDA to be used for coding. A two-parameter scatter plot (in Figure 7d) containing the fluorescence signals of QD-572 nm and QD-625 nm were obtained, in which the dots in the lower-left corner is PEGDA beads without QDs and the others represent the signal from PEGDA beads encoded by two color QDs with different concentration ratios. These remarkably distinguishable plots demonstrate the possible to use the resulted barcodes for high throughput detection.

ARTICLE

Journal Name

The feasibility of the resulted QD-encoded microspheres for suspension array was confirmed in a sandwich immunoassay for rabbit IgG (in Figure 8a). Goat anti-rabbit IgG used as capture antibody was tagged onto the surface

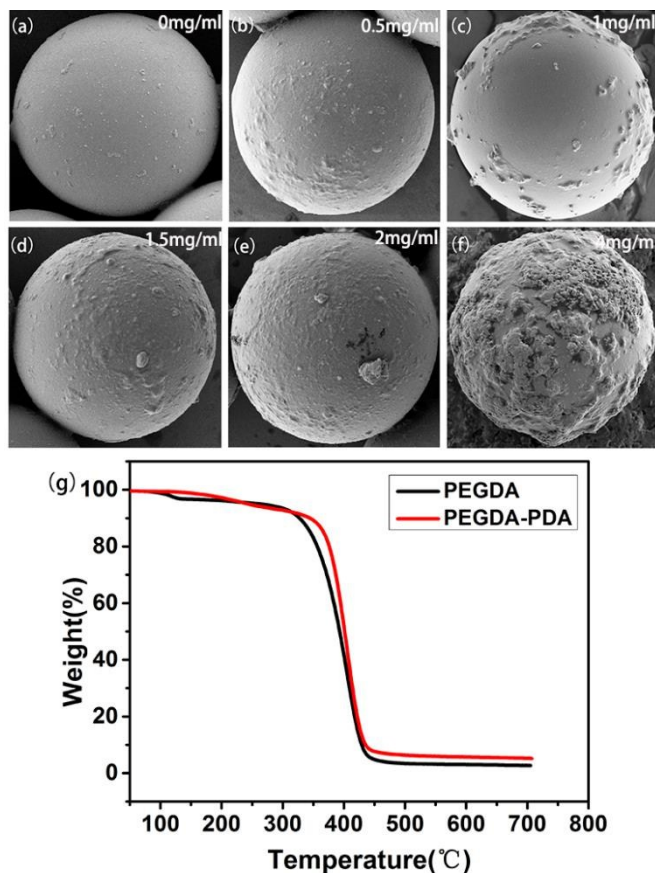


Figure 6. SEM images of PEGDA and PEGDA-PDA microspheres. (a) The pristine PEGDA microsphere. (b) – (f) The PEGDA-PDA composite beads modified with various concentrations of PDA: 0.5 mg/ml, 1 mg/ml, 1.5 mg/ml, 2 mg/ml and 4 mg/ml, respectively. (g) TGA curves of original PEGDA sphere (the black line) and PEGDA-PDA composite sphere (the red line).

of barcodes through the reaction of PDA and amine groups of the protein and BSA were attached on microbeads as non-specific binding control. The target molecule was rabbit IgG and the report molecule was the goat anti-rabbit IgG labeled by FITC. Here, the emission wavelength of QD-encoded microspheres was 625 nm, the barcodes were decoded by FL3 channel and FITC fluorescence was detected by FL1 channel. In Figure 8b, the fluorescence intensity comparison of BSA control group and FITC group in FL1 are significantly different, in which all the fluorescence intensities of QD-encoded beads were constant. The intensity of FITC group is higher than the BSA control group in Figure 8c. These results confirm the flexibility of PDA and indicate that immunoreactions between the capture antibodies on the surface of QD-encoded beads and antigens really occurred in this experiment.

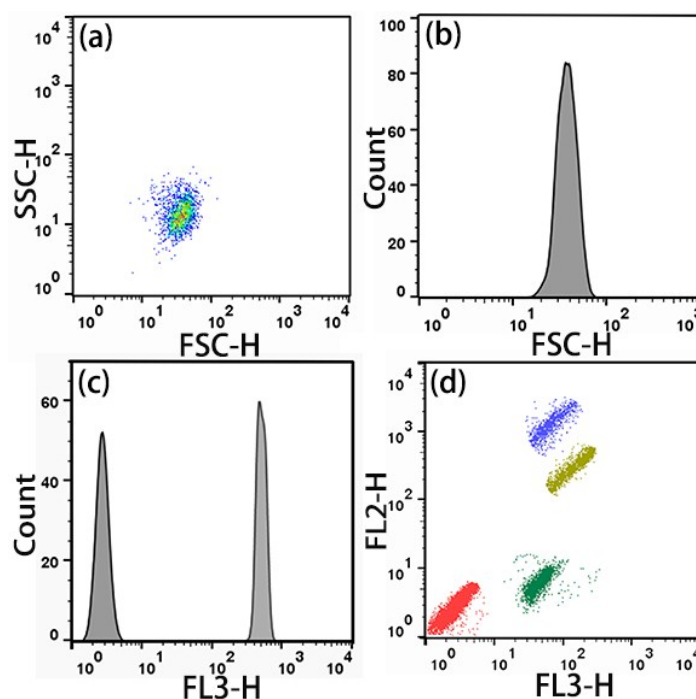


Figure 7. The flow cytometer analysis images of PEGDA barcodes. (a) Bead populations demonstrated by the picture of side light scatter (SSC) versus forward light scatter (FSC). (b) The histogram of size distribution. (c) The fluorescence signal (FL3) of PEGDA beads and QD-embedded PEGDA beads. (d) Plot of log FL2 versus log FL3 for barcodes.

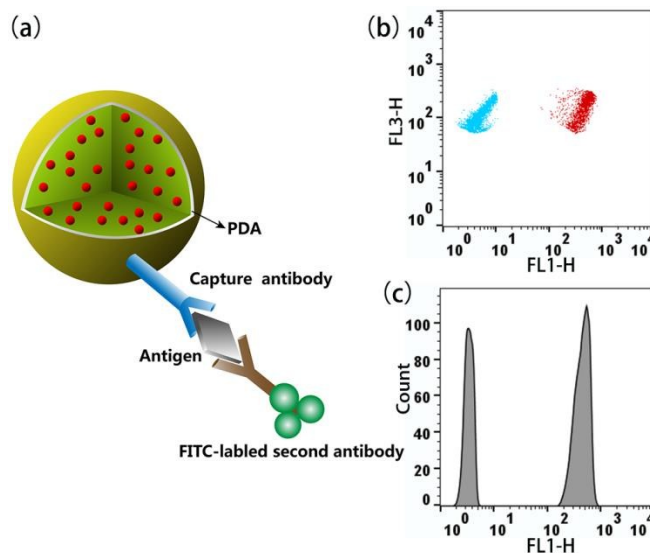


Figure 8. The diagram of QD-encoded bead-based immunoassays and flow cytometer analysis. (a) The sandwich immunoassay for detecting rabbit IgG. (b) Plot of the BSA control group and the FITC group. (c) The corresponding fluorescence intensity comparison.

Conclusions

In conclusion, we have developed a microfluidic approach to generate QD-encoded PEGDA barcodes with controlled sizes and accurate encoding signals. An S-shaped and gradually widening channel is designed to ensure sufficient UV exposure time for in-situ photopolymerization and prevents coalescence. The size range of the resulted PEGDA microbeads varied from 7 μm to 120 μm and show well-defined sphericity and excellent monodispersity with CV below 5 %. The mPEG-SH modified QDs were easily incorporated into the PEGDA beads by mixing them prior injection. The fluorescence performance of the embedded QDs is well reserved without significant peak broadening or distortion. Seven barcode libraries were realized and they presented bright fluorescence and distinguished coding signals and they could be conveniently decoded by a flow cytometer. In addition, PEGDA microspheres were modified with polydopamine (PDA), and this strategy offers a convenient way to conjugate capture molecules on the bead surface. A sandwich immunoassay for rabbit IgG detection was demonstrated. We envisage those fluorescence microbeads could find wide applications including multiplexed suspension assay in the future.

Acknowledgements

This work was supported by the National Natural Science Foundation of China (grants no. 21273126, 21573124) and Fundamental Research Program of Shenzhen (JCYJ20140509172959966).

References

- 1 L. Chin, J. N. Andersen, P. A. Futreal, *Nat. Med.*, 2011, **17**, 297-303.
- 2 N. G. Clack, K. Salaita, J. T. Groves, *Nat. Biotechnol.*, 2008, **26**, 825-830.
- 3 K. Braeckmans, S. C. De Smedt, M. Leblans, R. Pauwels, J. Demeester, *Nat. Rev. Drug Discov.*, 2002, **1**, 447-456.
- 4 Y. C. Cao, R. Jin, C. A. Mirkin, *Science*, 2002, **297**, 1536-1540.
- 5 G. MacBeath, S. L. Schreiber, *Science*, 2000, **289**, 1760-1763.
- 6 M. Y. Han, X. H. Gao, J. Z. Su, S. M. Nie, *Nat. Biotechnol.*, 2001, **19**, 631-635.
- 7 R. Wilson, A. R. Cossins, D. G. Spiller, *Angew. Chem. Int. Ed.*, 2006, **45**, 6104-6117.
- 8 M. T. Guo, A. Rotem, J. A. Heyman, D. A. Weitz, *Lab Chip*, 2012, **12**, 2146-2155.
- 9 Y. J. Zhao, Y. Cheng, L. R. Shang, J. Wang, Z. Y. Xie, Z. Z. Gu, *Small*, 2015, **11**, 151-174.
- 10 J. Neng, M. H. Harpster, W. C. Wilson, P. A. Johnson, *Biosens. Bioelectron.*, 2013, **41**, 316-321.
- 11 P. S. Eastman, W. Ruan, M. Doctolero, R. Nuttall, G. D. Feo, J. S. Park, J. S. F. Chu, P. Cooke, J. W. Gray, S. Li, F. F. Chen, *Nano Lett.*, 2006, **6**, 1059-1064.
- 12 G. Wang, Y. L. Leng, H. J. Dou, L. Wang, W. W. Li, X. B. Wang, K. Sun, L. S. Shen, X. L. Yuan, J. Y. Li, K. Sun, J. S. Han, H. S. Xiao, Y. Li, *ACS Nano.*, 2013, **7**, 471-48.
- 13 J. M. Nam, C. S. Thaxton, C. A. Mirkin, *Science*, 2003, **301**, 1884-1886.
- 14 D. C. Pregibon, M. Toner, P. S. Doyle, *Science*, 2007, **315**, 1393-1396.
- 15 Y. M. Lai, S. Q. Sun, T. Schlucker, S. He, Y. L. Wang, *RSC Adv.*, 2015, **5**, 13762-13767.
- 16 U. Resch-Genger, M. Grabolle, S. Cavaliere-Jaricot, R. Nitschke, T. Nann, *Nat. Methods*, 2008, **5**, 763-775;
- 17 J. Wang, Y. X. Liu, F. Peng, C. Y. Chen, Y. H. He, H. Ma, L. X. Cao, S. Q. Sun, *Small*, 2012, **8**, 2430-2435.
- 18 F. Li, J. Wang, S. Q. Sun, H. Wang, Z. Y. Tang, G. J. Nie, *Small*, 2015, **11**, 1954-1961.
- 19 M.D. Regulacio, M. Y. Han, *Acc. Chem. Res.*, 2010, **43**, 621-630.
- 20 T. Song, Q. Zhang, C. L. Lu, X. Q. Gong, Q. H. Yang, Y. H. Li, J. Q. Liu, J. Chang, *J. Mater. Chem.*, 2011, **21**, 2169-2177.
- 21 S. Rauf, A. Glidle, J. M. Cooper, *Adv. Mater.*, 2009, **21**, 4020-4024.
- 22 D. E. Gomez, I. S. Pastoriza, P. Mulvaney, *Small*, 2005, **1**, 238-241.
- 23 Y. H. Yang, Z. K. Wen, Y. P. Dong, M. Y. Gao, *Small*, 2006, **2**, 898-901.
- 24 Q. B. Wang, D. K. Seo, *J. Mater. Sci.*, 2009, **44**, 816-820.
- 25 S. K. Lee, J. Baek, K. F. Jensen, *Langmuir*, 2014, **30**, 2216-2222.
- 26 K. Q. Jiang, C. Xue, C. D. Arya, C. R. Shao, E. O. George, D. L. DeVoe, S. R. Raghavan, *Small*, 2011, **7**, 2470-2476.
- 27 I. Lee, Y. Yoo, Z. D. Cheng, H. K. Jeong, *Adv. Funct. Mater.*, 2008, **18**, 4014-4021.
- 28 Y. J. Zhao, H. C. Shum, H. S. Chen, L. L. A. Adams, Z. Z. Gu, D. A. Weitz, *J. Am. Chem. Soc.*, 2011, **133**, 8790-8793.
- 29 S. Fournier-Bidoz, T. L. Jennings, J. M. Klostianec, W. Fung, A. Rhee, D. Li, W. C. W. Chan, *Angew. Chem. Int. Ed.*, 2008, **47**, 5577-5663.
- 30 Y. Chen, P. F. Dong, J. H. Xu, G. S. Luo, *Langmuir*, 2014, **30**, 8538-8542.
- 31 C. H. Yang, K. S. Huang, Y. S. Lin, K. Lu, C. C. Tzeng, E. C. Wang, C. H. Lin, W. Y. Hsu, J. Y. Chang, *Lab Chip*, 2009, **9**, 961-965.
- 32 H. Liu, G. H. Li, X. Y. Sun, Y. H. He, S. Q. Sun, H. Ma, *RSC Adv.*, 2015, **5**, 62706-62712.
- 33 X. H. Ji, N. G. Zhang, W. Cheng, F. Guo, W. Liu, S. S. Guo, Z. K. He, X. Z. Zhao, *J. Mater. Chem.*, 2011, **21**, 13380-13387.
- 34 X. H. Ji, W. Cheng, F. Guo, W. Liu, S. S. Guo, Z. K. He, X. Z. Zhao, *Lab Chip*, 2011, **11**, 2561-2568.
- 35 H. Lee, S. M. Dellatore, W. M. Miller, P. B. Messersmith, *Science*, 2007, **318**, 426-430.
- 36 Y. Cong, T. Xia, M. Zou, Z. N. Li, B. Peng, D. Z. Guo, Z. W. Deng, *J. Mater. Chem. B*, 2014, **2**, 3450-3461.
- 37 F. Gao, H. Qu, Y. Duan, J. Wang, X. Song, T. B. Ji, L. X. Cao, G. J. Nie, S. Q. Sun, *RSC Adv.*, 2014, **4**, 6657-6663.

Graphical Abstract:

A simple microfluidic device is designed to generate monodispersed QD-encoded PEGDA microbeads. PEGDA/PDA composite microspheres are prepared to easily couple protein on their surface. A sandwich immunoassay of rabbit IgG is performed to indicate that PDA on the bead surface facilitate efficient attachment of biomacromolecules.

